

Electronic Supplementary Information

Metal-Organic Framework with Tunable Exposed Facets as a High-affinity Artificial Receptor for Enzyme Inhibition

Ming Xu^{†,‡}, Sha-Sha Meng^{†,‡}, Hong Liang[†] and Zhi-Yuan Gu^{,†}*

[†]Jiangsu Key Laboratory of Biofunctional Materials, Jiangsu Collaborative Innovation Center of Biomedical Functional Materials, College of Chemistry and Materials Science, Nanjing Normal University, Nanjing, 210023, China

*Corresponding author: guzhiyuan@njnu.edu.cn

[‡] Ming Xu and Sha-Sha Meng contributed equally

Contents

Section S1. Chemicals and Instrumentation	3
Section S2. Catalytic Triad of ChT	4
Section S3. Characterization of HKUST-1	5
Section S4. Activity of HKUST-1	6
Section S5. Activity of ChT with Different Standing Time	7
Section S6. Activity of ChT with the Incubation of HKUST-1 for Different Time	8
Section S7. Dynamic Light Scattering of HKUST-1	9
Section S8. Activity of ChT with Different Concentrations of HKUST-1	10
Section S9. Activity of ChT with or without the Incubation of HKUST-1 at Different Concentrations of Substrate	11
Section S10. Activity of ChT with the Incubation of HKUST-1 in Different Buffers	12
Section S11. Activity of ChT with the Incubation of HKUST-1 in the Presence of NaCl at Different Concentrations.	14
Section S12. Activity of ChT with the Incubation of other MOFs	16
Section S13. Activity of ChT with the Incubation of HKUST-1 in the Presence of Histidine at Different Concentrations	17
Section S14. Fluorescence of ChT with and without Incubation with HKUST-1	19
Section S15. Synthesis and the Characterization of HKUST-1 with Exclusively {100} Facets	20
Section S16. Synthesis of HKUST-1 with Different Exposed Facets	22
Section S17. Calculation of Half Maximal Inhibitory Concentration (IC_{50}) for ChT	25
Section S18. Activity of ChT with the Incubation of BTC Ligands	29

Section S1. Chemicals and Instrumentation

All chemicals employed were of analytical grade and used as supplied without further purification. The $\text{Cu}(\text{NO}_3)_2 \cdot 3\text{H}_2\text{O}$, 1,3,5-benzenetricarbocyclic acid, 1,3,5-benzenetricarbocyclic acid, 4-(2-hydroxyethyl)-1-piperazinepropanesulfonic acid (HEPPS), piperazine-N,N'-bis(2-ethanesulfonic acid) (PIPES), 4-(2-hydroxyethyl)piperazine-1-(2-hydroxypropanesulfonic acid) (HEPPSO), NaOH, lauric acid (LA) and dimethyl sulfoxide (DMSO) were purchased from Aladdin Industrial Inc (Shanghai, China). N-succinyl-L-phenylalanine-p-nitroanilide (SPNA) was purchased from Sigma (St. Louis, MO). α -Chymotrypsin (ChT) was purchased from Sangon Biotech (Shanghai) Co., Ltd (Shanghai, China). Ethanol (EtOH) was purchased from Sinopharm Chemical Reagent Co., Ltd (Shanghai, China). Powder X-ray diffraction (PXRD) patterns were obtained from Rigaku D/MAX-2500 diffractometer with a $\text{CuK}\alpha$ radiation (1.54056 Å). Transmission electron microscopy (TEM) analyses were performed on JEOL JEM-2100F transmission electron microscopy operated at an accelerating voltage of 200 kV. Scanning electron microscope (SEM) images were collected on a JSM-7600F (JEOL Ltd) scanning electron microscope. Zeta potential and dynamic light scattering (DLS) measurements were made with a Malvern Zetasizer NANO-ZS90.

Section S2. Catalytic Triad of ChT

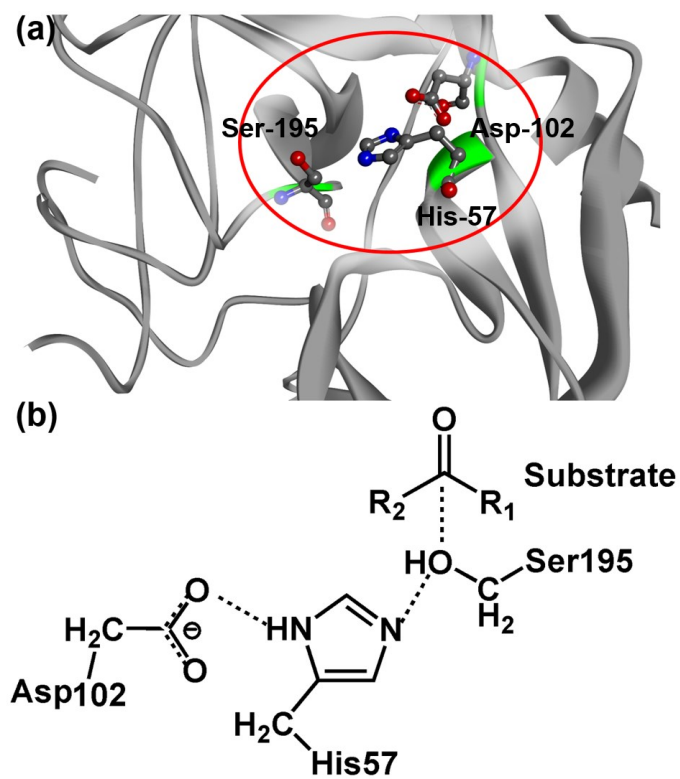


Figure S1. (a) Molecular structure of ChT. Polychrome sections in this structure are the active site with residues of Asp-102, His-57, and Ser-195. (b) Substrate and three active residues (catalytic triad) in the active site of ChT.

Section S3. Characterization of HKUST-1

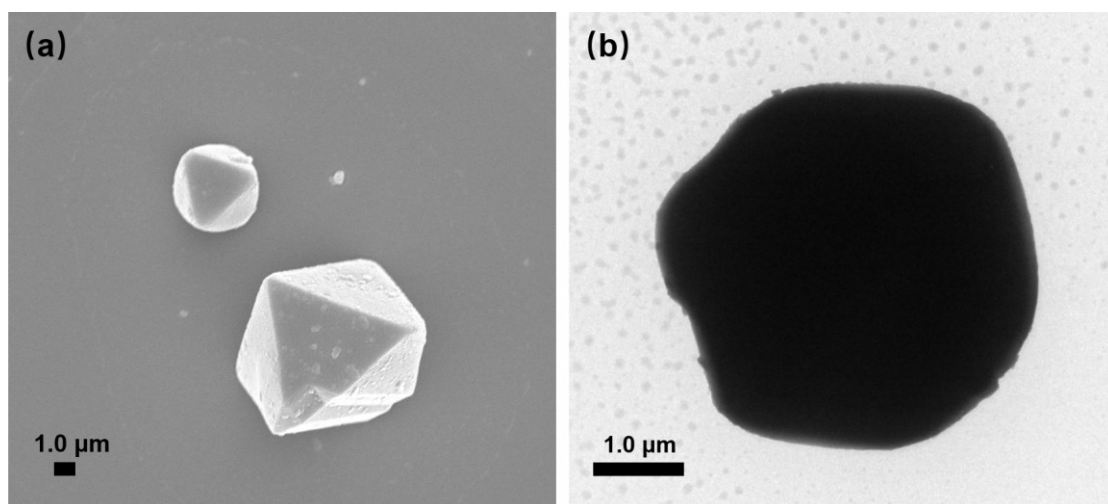


Figure S2. SEM (a) and TEM (b) images of HKUST-1.

Section S4. Activity of HKUST-1

The HKUST-1 was dissolved with HEPPS buffer (100 mM, pH = 7.4). To obtain the activity of HKUST-1, the substrate (SPNA, 160 μ L) was added to the HKUST-1 suspension solution (30 μ g/mL, 1840 μ L). The concentration of SPNA was 2 mM in the solvent mixture of ethanol/DMSO (90%/10%). Enzyme activity was collected by monitoring the absorbance of PNA every 2 min for 20 min in 30 $^{\circ}$ C at 410 nm with Hitachi UH5300 spectrophotometer. For comparison, the activity of ChT (80 μ g/mL) was monitored as well.

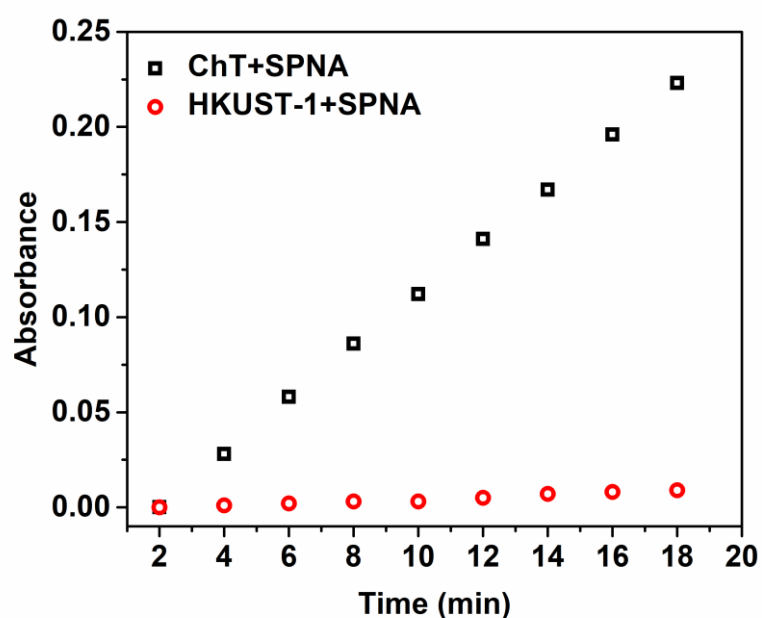


Figure S3. Activity of HKUST-1 (30 μ g/mL, red symbol) and activity of ChT (80 μ g \cdot mL $^{-1}$, black symbol).

Section S5. Activity of ChT with Different Standing Time

The ChT was dissolved with HEPPS buffer (100 mM, pH = 7.4). To obtain the activity of ChT, the substrate (SPNA, 160 μ L) was added to the ChT solution (1840 μ L). The concentration of SPNA was 2 mM in the solvent mixture of ethanol/DMSO (90%/10%). Enzyme activity was collected by monitoring the absorbance of PNA every 2 min for 20 min at 410 nm with Hitachi UH5300 spectrophotometer. Herein, ChT was incubated in a 30 $^{\circ}$ C water bath for different time and then used for the activity measurement.

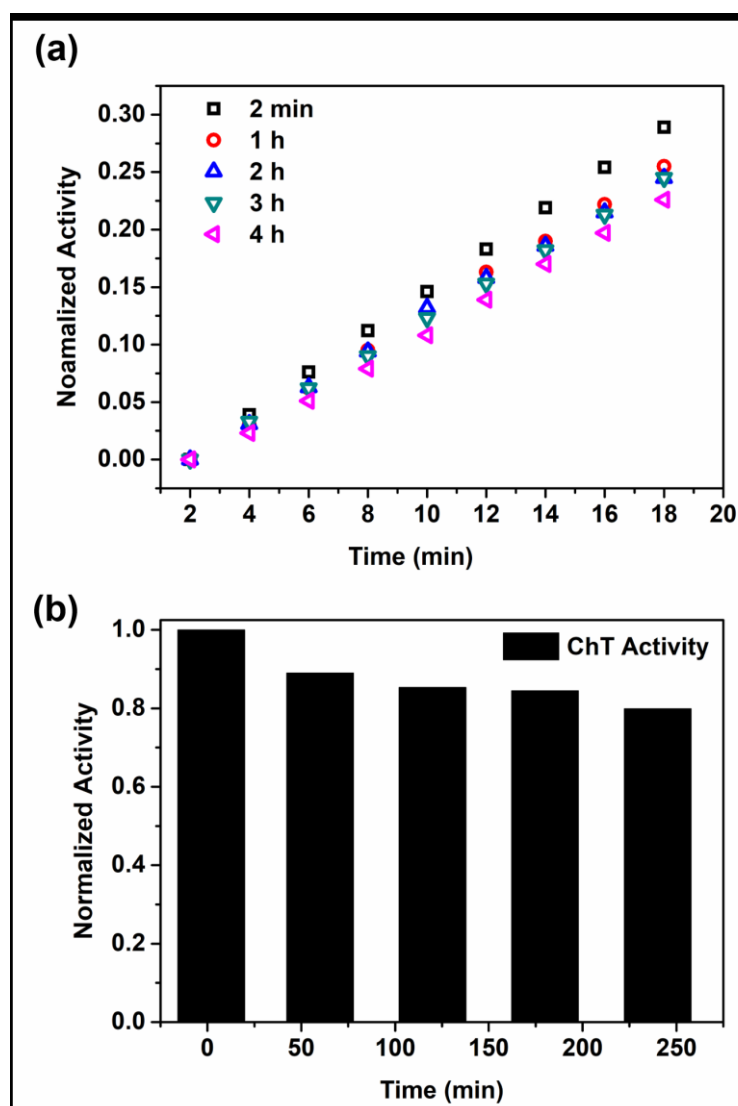


Figure S4. (a) Activity of ChT ($80 \mu\text{g}\cdot\text{mL}^{-1}$) with different standing time (2 min, 60 min, 120 min, 180 min and 240 min). (b) Enzymatic activity was normalized to that of ChT at 2 min.

Section S6. Activity of ChT with the Incubation of HKUST-1 for Different Time

All of the substances were dissolved in HEPPS buffer (100 mM, pH = 7.4) at 30 °C. ChT was incubated with HKUST-1 (30 $\mu\text{g/mL}$) solution for different time. To obtain the activity of ChT, the substrate (SPNA, 160 μL) was added to the MOF-ChT solution (1840 μL). The concentration of SPNA was 2 mM in the solvent mixture of ethanol/DMSO (90%/10%). Enzyme activity was collected by monitoring the absorbance of PNA every 2 min for 20 min at 410 nm with a Hitachi UH5300 spectrophotometer.

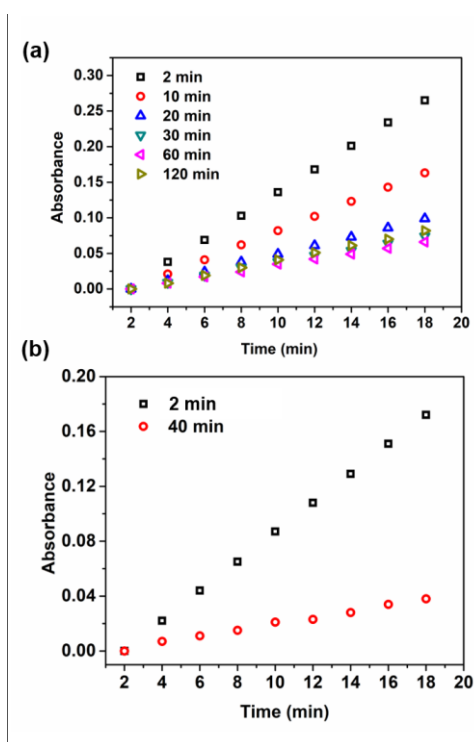


Figure S5. (a) Activity of ChT (80 $\mu\text{g/mL}$) with the incubation of HKUST-1 (30 $\mu\text{g/mL}$) for different time (2 min, 10 min, 20 min, 30 min, 60 min and 120 min). (b) Activity of ChT (80 $\mu\text{g/mL}$) with the incubation of HKUST-1 (30 $\mu\text{g/mL}$) for different time (2 min and 40 min). The low ChT activity without HKUST-1 in (b) resulted from the denaturing of the stored ChT because the experiments were conducted half a year after the experiments in (a). All the inhibition efficiency was calculated through normalizing the ChT activity with inhibitors to the corresponding ChT activity without inhibitors. Thus, it would not influence our conclusion.

Section S7. Dynamic Light Scattering of HKUST-1

The aggregation of HKUST-1 was confirmed by the DLS results. Typically, different concentrations of HKUST-1 (30 $\mu\text{g/mL}$ and 100 $\mu\text{g/mL}$) was added into the ChT solution (80 $\mu\text{g/mL}$). Then, the mixture was kept standing for different time (10 min, 30 min and 120 min). DLS measurements were made with a Malvern Zetasizer NANO-ZS90.

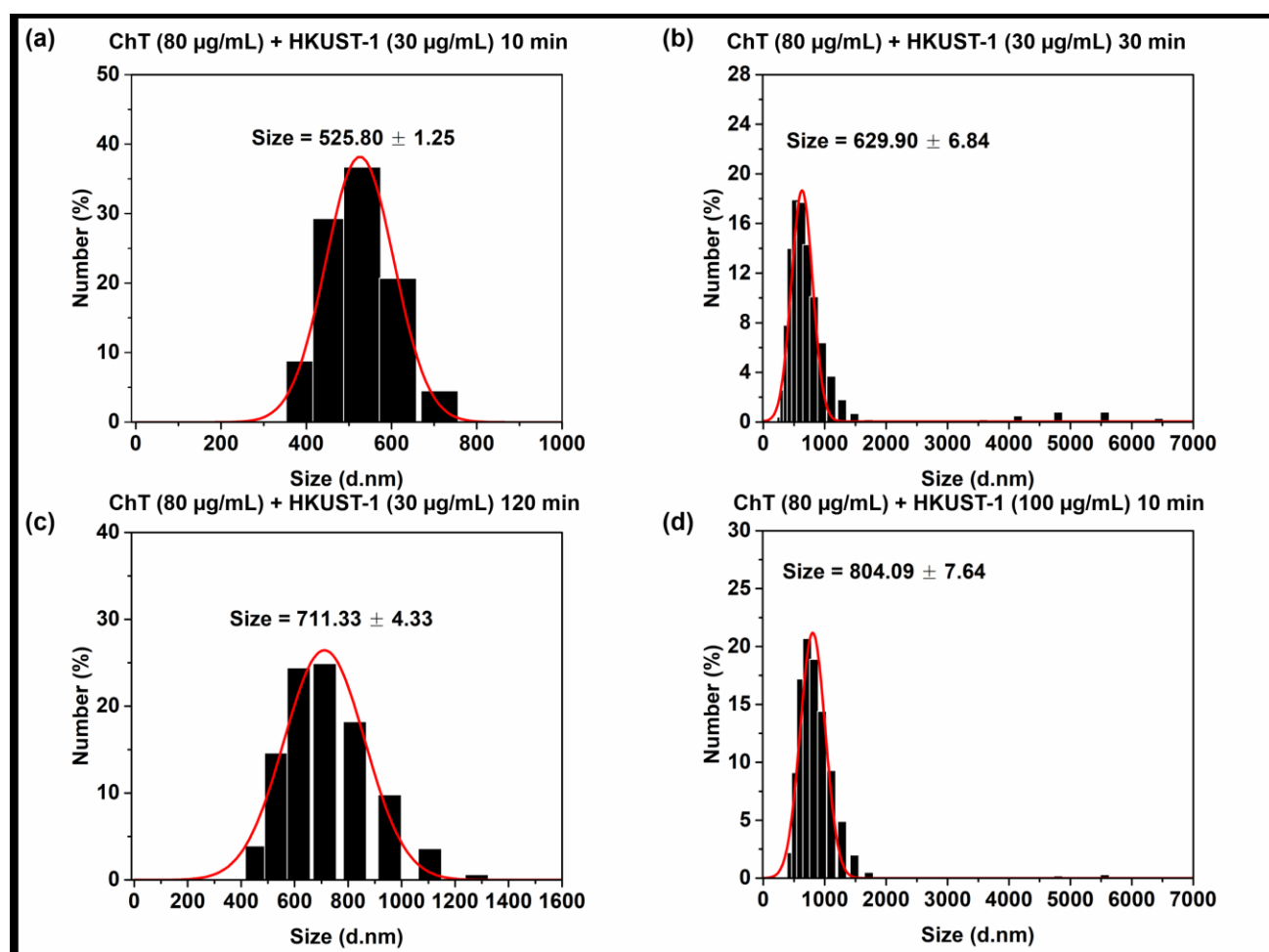


Figure S6. (a) DLS results of the ChT (80 $\mu\text{g/mL}$) and HKUST-1 (30 $\mu\text{g/mL}$) mixture after incubation for 10 min. (b) DLS results of the ChT (80 $\mu\text{g/mL}$) and HKUST-1 (30 $\mu\text{g/mL}$) mixture after incubation for 30 min. (c) DLS results of the ChT (80 $\mu\text{g/mL}$) and HKUST-1 (30 $\mu\text{g/mL}$) mixture after incubation for 120 min. (d) DLS results of the ChT (80 $\mu\text{g/mL}$) and HKUST-1 (100 $\mu\text{g/mL}$) mixture after incubation for 10 min.

Section S8. Activity of ChT with Different Concentrations of HKUST-1

Activity of ChT was detected with the similar method as in section S4 and S5. The ChT (80 $\mu\text{g/mL}$) was incubated with HKUST-1 for 10 min. The concentrations of HKUST-1 varied from 0 to 100 $\mu\text{g/mL}$.

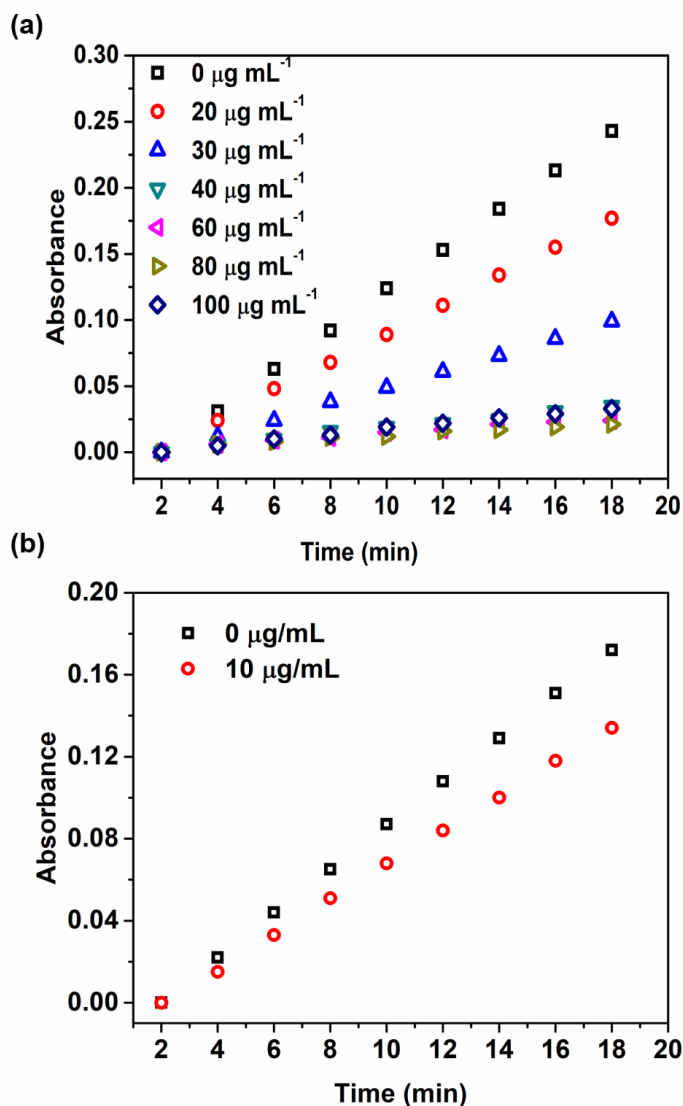


Figure S7. (a) Activity of ChT (80 $\mu\text{g/mL}$) with different HKUST-1 concentrations (0, 20, 30, 40, 60, 80 and 100 $\mu\text{g/mL}$). (b) Activity of ChT (80 $\mu\text{g/mL}$) with different HKUST-1 concentrations (0 and 10 $\mu\text{g/mL}$). The low ChT activity without HKUST-1 in (b) resulted from the denaturing of the stored ChT, because the experiments were conducted half a year after the experiments in (a). All the inhibition efficiency was calculated through normalizing the ChT activity with inhibitors to the corresponding ChT activity without inhibitors. Thus, it would not influence our conclusion.

Section S9. Activity of ChT with or without the Incubation of HKUST-1 at Different Concentrations of Substrate

Activity of ChT was detected with the similar method as in section S4 and S5. The ChT was incubated without or with HKUST-1 (30 $\mu\text{g/mL}$) solution for 10 min. The concentrations of SPNA varied from 1 to 5 mM in the solvent mixture of ethanol/DMSO (90%/10%).

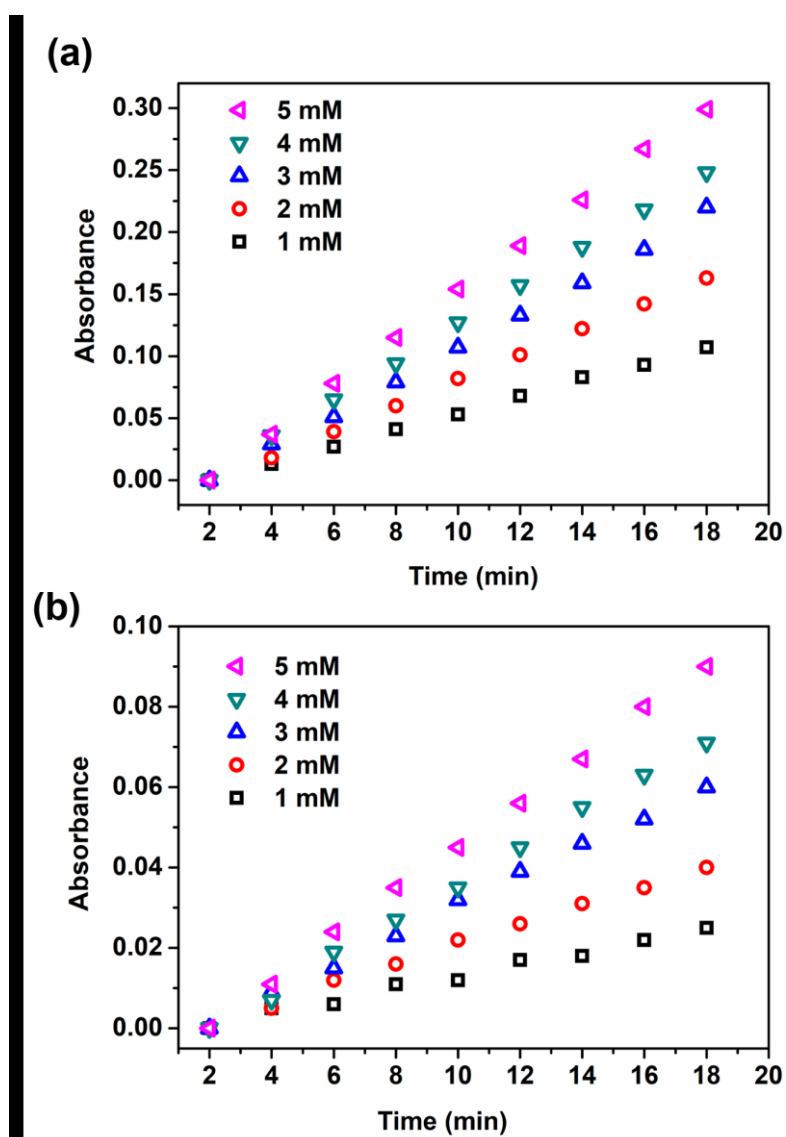


Figure S8. Activity of ChT (80 $\mu\text{g/mL}$) without (a) and with (b) the incubation of HKUST-1 (30 $\mu\text{g/mL}$) at different concentrations of substrate SPNA.

Section S10. Activity of ChT with the Incubation of HKUST-1 in Different Buffers

Activity of ChT was detected with the similar method as in section S4 and S5. The ChT was incubated without or with HKUST-1 (30 $\mu\text{g/mL}$) solution for 10 min. The buffers were changed from HEPPS (100 mM, pH = 7.4) to HEPPSO (100 mM, pH = 7.4) and PIPES (100 mM, pH = 7.4).

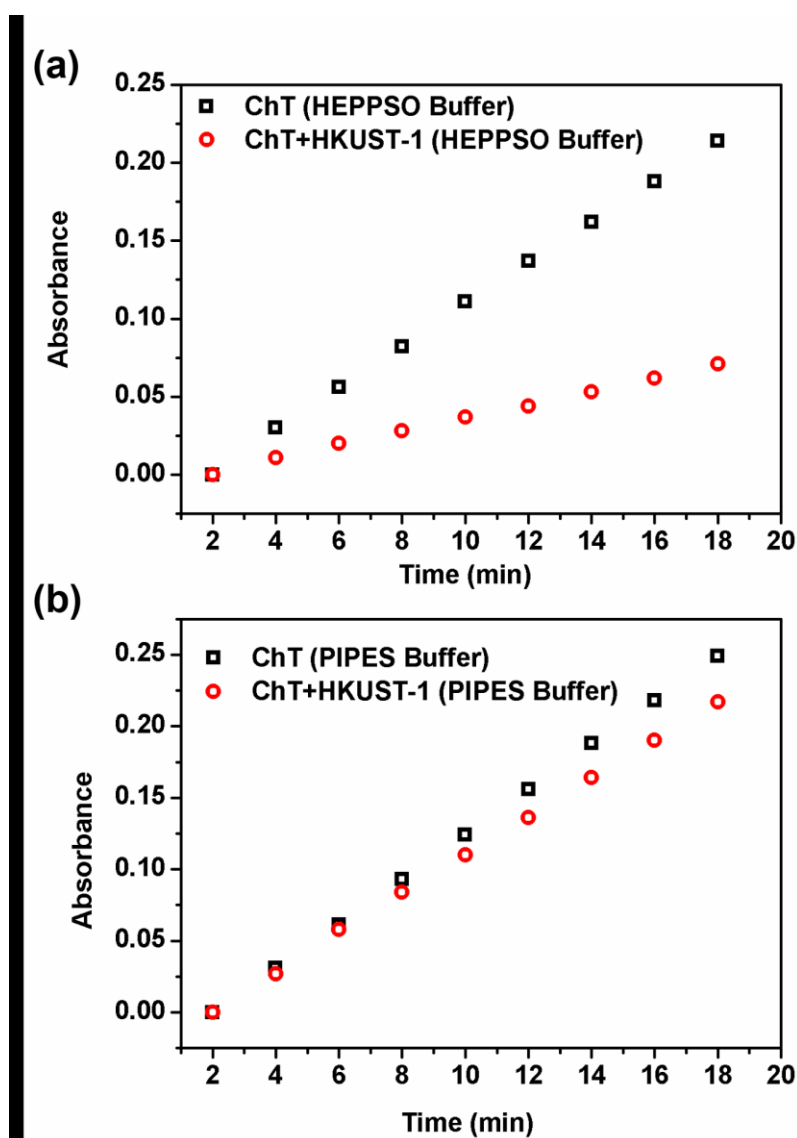


Figure S9. Activity of ChT (80 $\mu\text{g/mL}$) incubated without and with HKUST-1 (30 $\mu\text{g/mL}$) in (a) HEPPSO and (b) PIPES buffers.

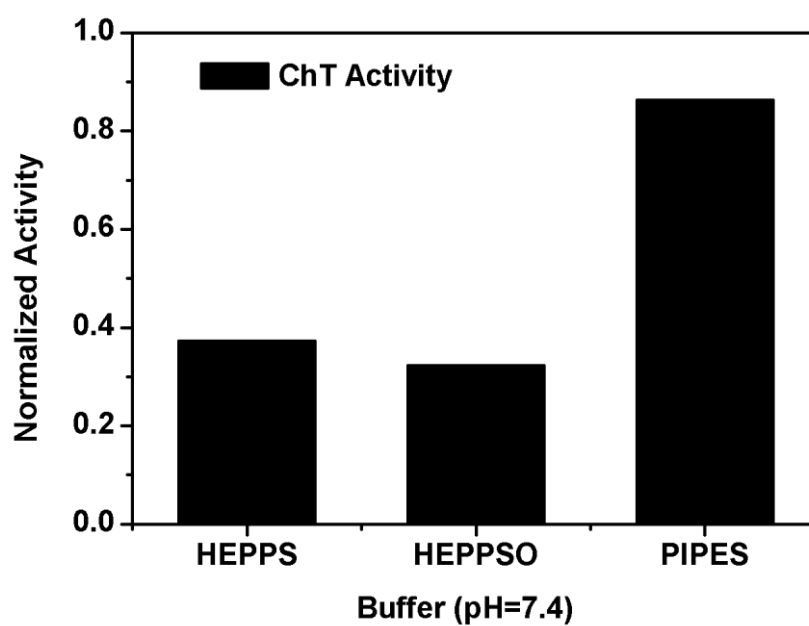


Figure S10. Activity of ChT (80 µg/mL) incubated with HKUST-1 (30 µg/mL) in different buffers. The activity was normalized to the ChT activity without the incubation of HKUST-1 in the corresponding buffers.

Section S11. Activity of ChT with the Incubation of HKUST-1 in the Presence of NaCl at Different Concentrations.

Activity of ChT was detected with the similar method as in section S4 and S5. All of the substances were dissolved in HEPPS buffer (100 mM, pH = 7.4) at 30°C. Different concentrations of NaCl were added to 80 µg/mL ChT either before the addition of 40 µg/mL HKUST-1 (before incubation) or after the 10 min incubation with 40 µg/mL HKUST-1 (after incubation). The concentration of NaCl varied from 0 to 600 mM in 100 mM HEPES buffer (pH = 7.4). For comparison, the same series of NaCl were added to 80 µg/mL ChT without HKUST-1 and the activity was recorded as well.

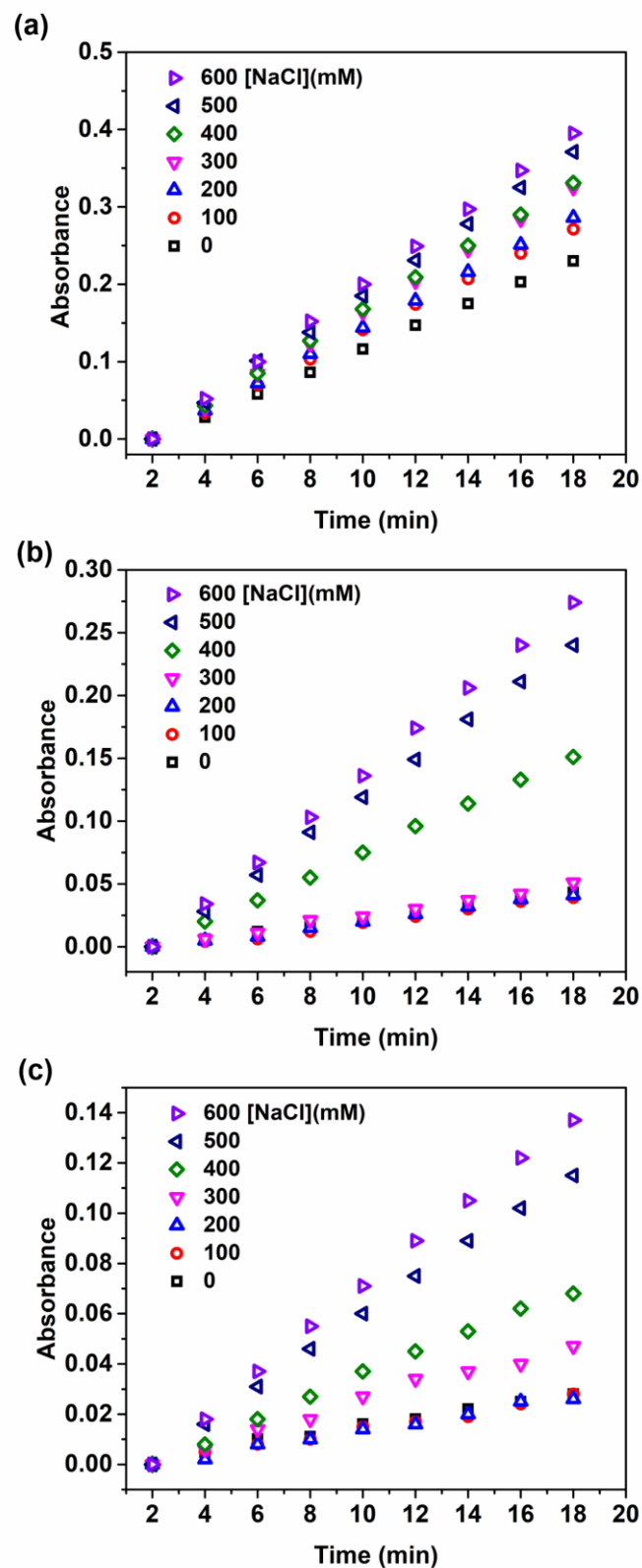


Figure S11. (a) Activity of ChT (80 μ g/mL) with different concentrations of NaCl in the absence of inhibitors. Activity of ChT (80 μ g/mL) with different concentrations of NaCl before (b) and after incubation (c) with HKUST-1 (40 μ g/mL) as an inhibitor.

Section S12. Activity of ChT with the Incubation of other MOFs

Herein, NTU-9 (Ti), UiO-66 (Zr) and MIL-125 (Ti) were synthesized according to the reported articles.¹⁻³ The ChT activity was detected with the similar method as in section S4 and S5. The ChT (80 $\mu\text{g/mL}$) was incubated with different MOFs for 10 min. The concentration of each MOF was fixed as 80 $\mu\text{g/mL}$.

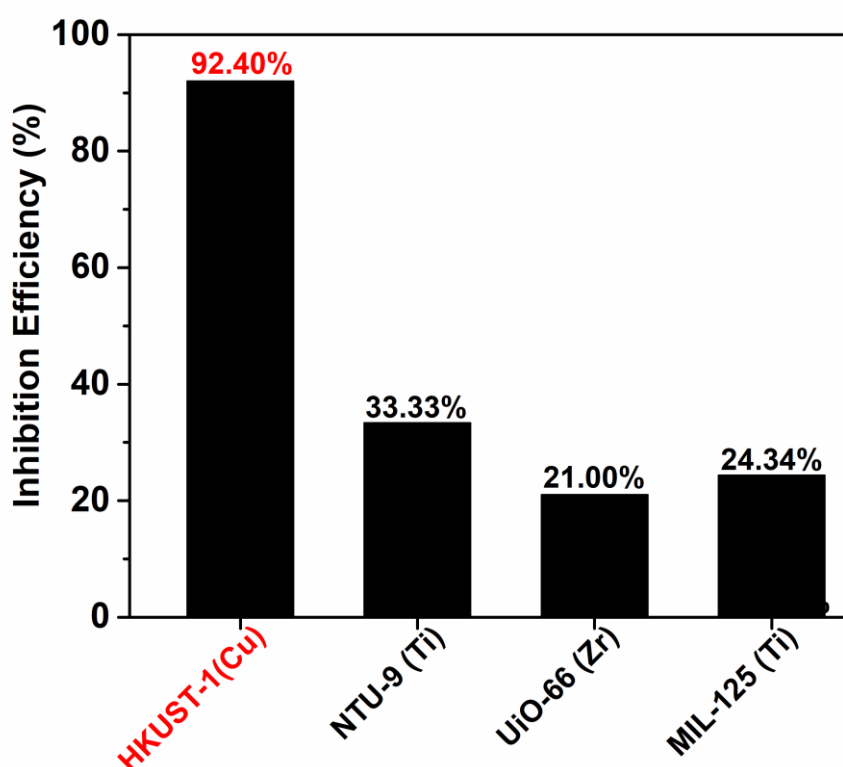


Figure S12. Activity of ChT (80 $\mu\text{g/mL}$) with the incubation of different MOFs (80 $\mu\text{g}\cdot\text{mL}^{-1}$).

Table S1. Zeta potential of different MOFs in pH 7.4 HEPPS buffer

MOFs	HKUST-1	NTU-9	UiO-66	MIL-125 (Ti)
Zeta potential (mV)	-14.0	-36.9	-32.0	-39.5

Section S13. Activity of ChT with the Incubation of HKUST-1 in the Presence of Histidine at Different Concentrations.

The ChT activity was detected with the similar method as in section S4 and S5. All of the substances were dissolved in HEPPS buffer (100 mM, pH = 7.4) at 30 °C. Different concentrations of histidine were added to 80 µg/mL ChT after the 10 min incubation with 40 µg/mL HKUST-1. The concentration of histidine varied from 0 to 600 µM in 100 mM HEPES buffer (pH = 7.4). For comparison, the catalysis activity of 600 µM histidine and the activity of ChT with 600 µM histidine without the inhibitor were recorded as well.

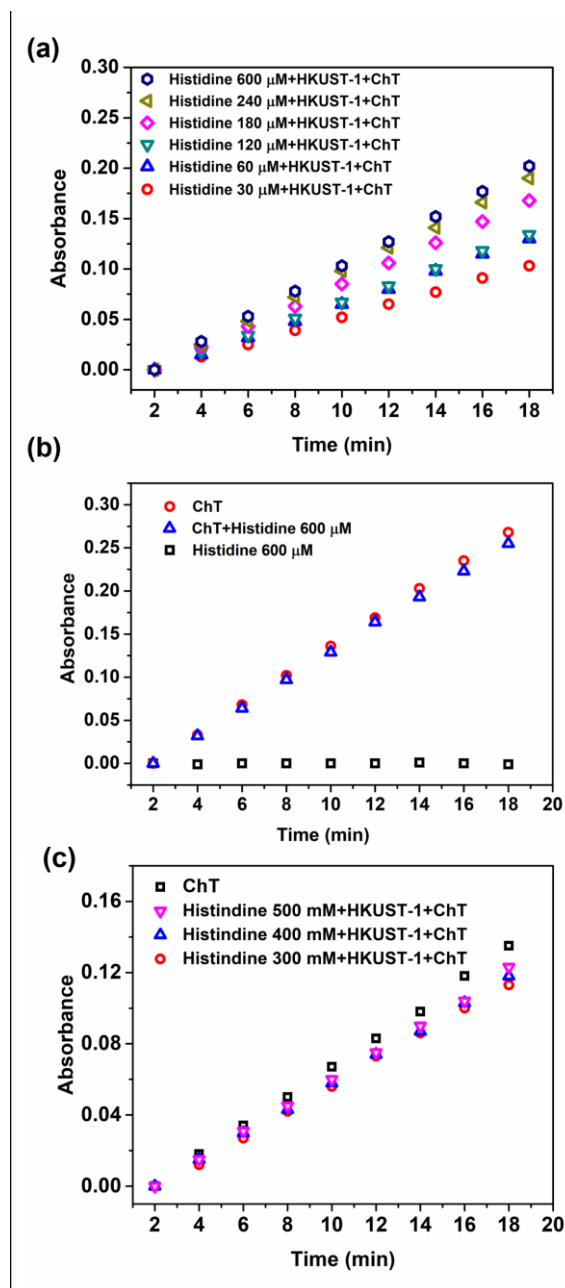


Figure S13. (a) Activity of ChT (80 $\mu\text{g/mL}$) with different concentrations of histidine in the presence of HKUST-1 (40 $\mu\text{g/mL}$). (b) Activity of ChT (80 $\mu\text{g/mL}$) with and without 600 μM histidine, as well as the activity of 600 μM histidine without MOFs and ChT. (c) Activity of ChT (80 $\mu\text{g/mL}$) with different concentrations of histidine with and without HKUST-1 (40 $\mu\text{g/mL}$). The low ChT activity without HKUST-1 in (c) resulted from the denaturing of the stored ChT because the experiments were conducted half a year after the experiments in (a) and (b). All the inhibition efficiency was calculated through normalizing the ChT activity with inhibitors to the corresponding ChT activity without inhibitors. Thus, it would not influence our conclusion.

Section S14. Fluorescence of ChT with and without Incubation with HKUST-1

1

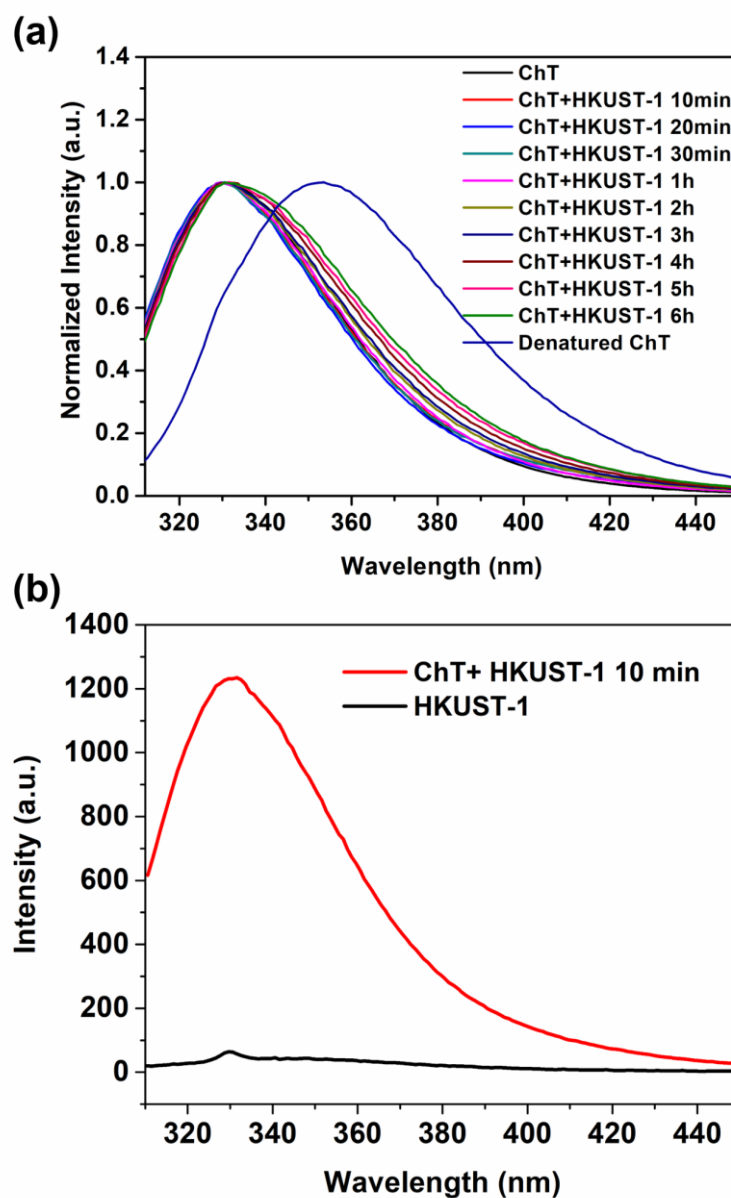


Figure S14. (a) Tryptophan fluorescence of ChT (80 $\mu\text{g/mL}$) with and without HKUST-1 (40 $\mu\text{g/mL}$) as an inhibitor for 10 min, 20 min, 30 min, 1 h, 2 h, 3 h, 4 h, 5 h and 6 h. The fluorescence of denatured ChT (80 $\mu\text{g/mL}$) was also recorded. The fluorescence intensity was normalized to the intensity of ChT without the inhibitors. (b) Fluorescence of HKUST-1 (40 $\mu\text{g/mL}$).

Section S15. Synthesis and the Characterization of HKUST-1 with Exclusively {100} Facets

Synthesis of HKUST-1 with more {100} facets

HKUST-1 was synthesized based on the reported paper with a few changes.⁴ Typically, $\text{Cu}(\text{NO}_3)_2 \cdot 3\text{H}_2\text{O}$ (41 mg) was dissolved in 10 mL n-butyl alcohol and lauric acid (0 mg, 475.5 mg, 951 mg, 1.4275 g, 1.902 g, 2.3775 g) was added into it. The dispersion was heated and stirred to form a clear solution. Then, H_3BTC (20 mg) was dissolved into the solution. After stirring for 10 min, the mixture was poured into a Teflon reaction kettle and heated at 120 °C for 24 h. The blue product HKUST-1 was collected by centrifugation and washed with ethanol for three times. After that, the HKUST-1 was dried at 60 °C overnight in a vacuum oven.

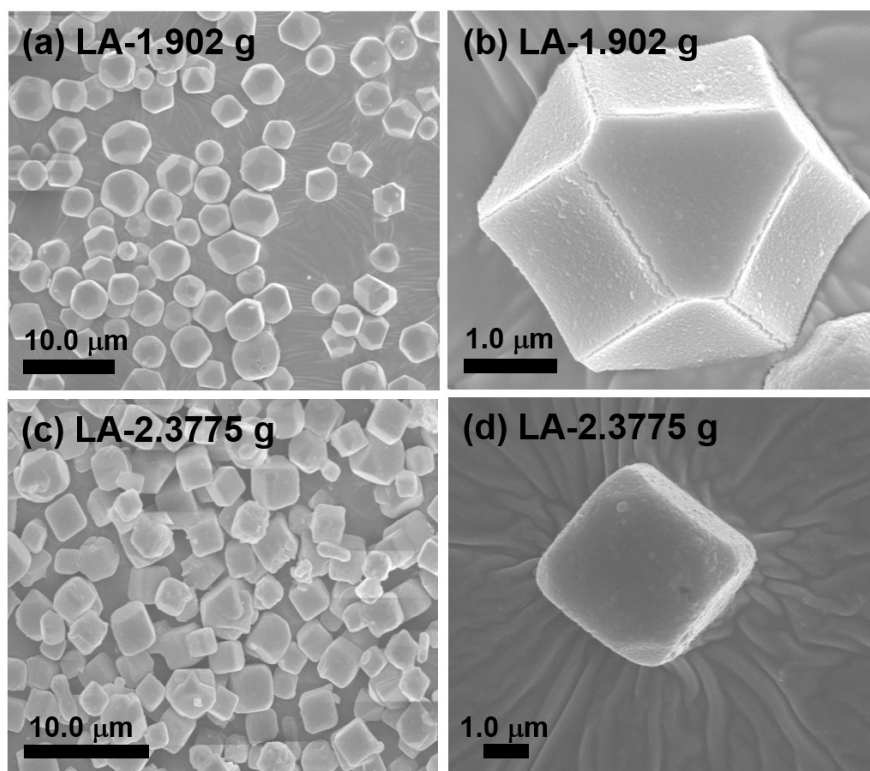


Figure S15. SEM images of HKUST-1 with more {100} facets.

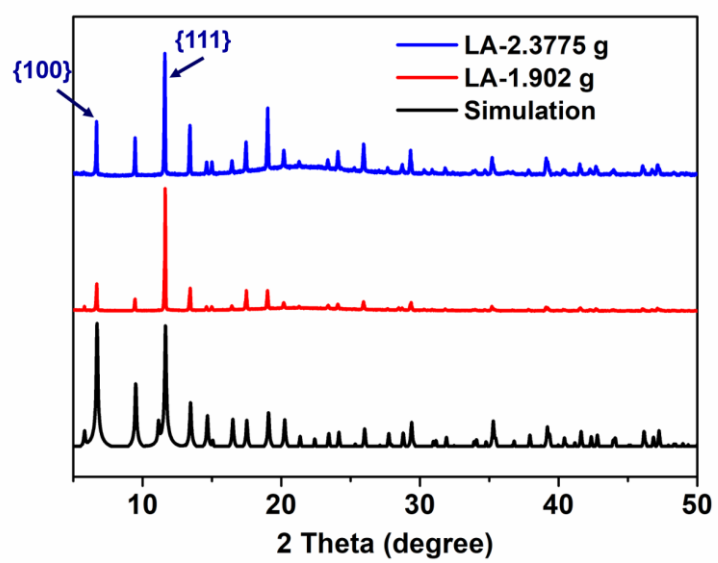


Figure S16. PXRD patterns of HKUST-1 with more {100} facets.

Section S16. Synthesis of HKUST-1 with Different Exposed Facets

With water as modulators

A series of HKUST-1 with different exposed facets were synthesized according to the reported method with few changes.⁵ Typically, 0.88 g $\text{Cu}(\text{NO}_3)_2 \cdot 3\text{H}_2\text{O}$ was dissolved in 15 mL ethanol and 0.42 g H_3BTC was dissolved in 12 mL water and ethanol mixture. In the 12 mL mixture, the moisture content varied from 30%, 40%, 50%, 60%, 70% to 90%. The solution of $\text{Cu}(\text{NO}_3)_2 \cdot 3\text{H}_2\text{O}$ and the solution of H_3BTC were mixed and stirred for 1 h at room temperature. Then, the mixture was poured into a Teflon reaction kettle and heated at 120 °C for 24 h. The blue product HKUST-1 was collected by centrifugation and washed with ethanol/water solution (the same volume ratio as the H_3BTC solution) for three times. After that, the HKUST-1 was dried at 60 °C overnight in a vacuum oven.

With NaOH as modulators

A series of HKUST-1 with different exposed facets were synthesized according to the reported method with few changes.⁶ Typically, 0.88 g (3.6 mmol) $\text{Cu}(\text{NO}_3)_2 \cdot 3\text{H}_2\text{O}$ was dissolved in 15 mL water and 0.42 g (2.0 mmol) H_3BTC was dissolved in 12 mL ethanol. The two solutions were mixed, and then the NaOH solution with different concentrations from 1 mmol, 2 mmol and 4 mmol was added, stirring for 1 h at room temperature. The mixture was poured into a Teflon reaction kettle and heated at 120 °C for 24 h. The blue product HKUST-1 was collected by centrifugation and washed with ethanol/water (50%/50%) solution for three times. After that, the HKUST-1 was dried at 60 °C overnight in a vacuum oven.

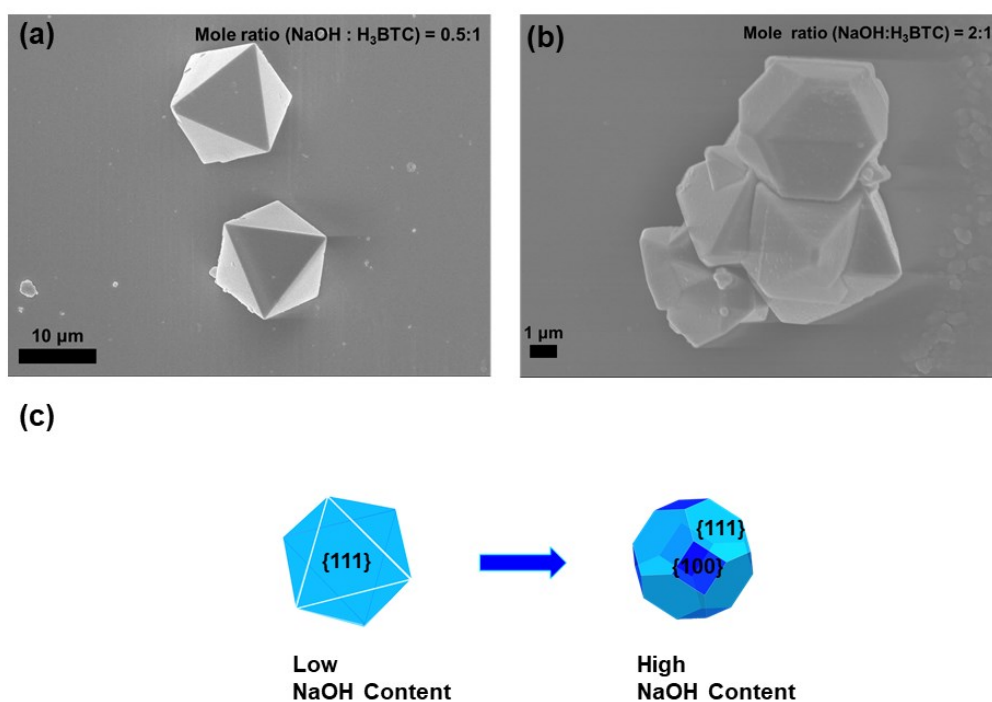


Figure S17. (a-b) TEM images of HKUST-1 with NaOH as modulators. (d) A schematic illustration of the exposed facets changes of HKUST-1 with NaOH as modulators.

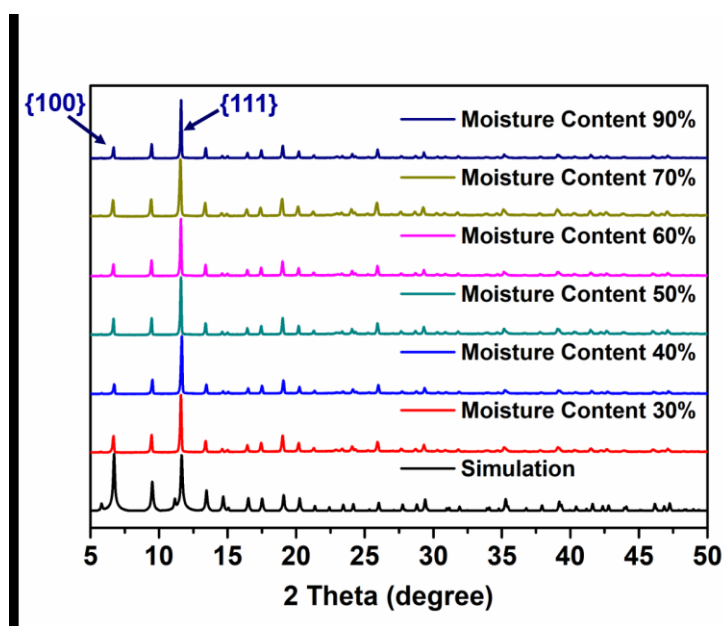


Figure S18. PXRD patterns of HKUST-1 with water as modulators.

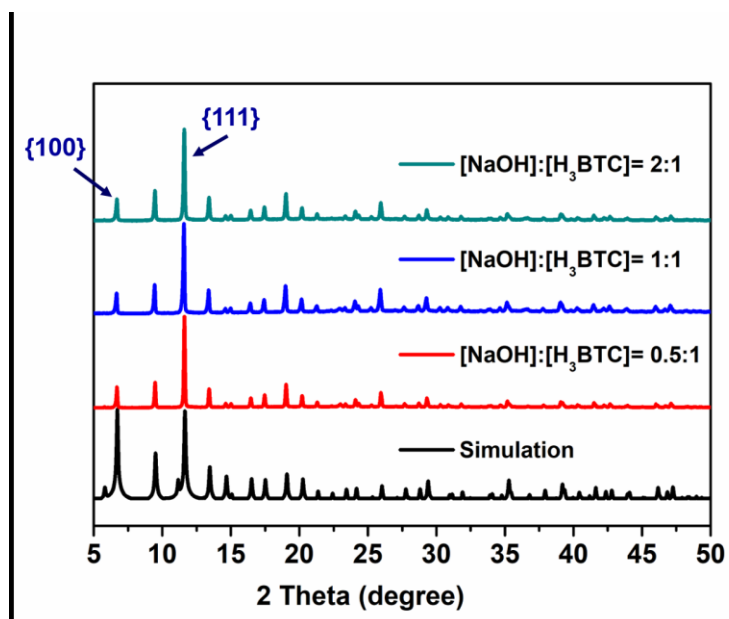


Figure S19. PXRD patterns of HKUST-1 with NaOH as modulators. The PXRD patterns performed no difference, which indicated that the HKUST-1 was successfully synthesized. While, the diffraction peak of different facets exhibited almost no difference, which might result from the poor recognition of PXRD. The phenomenon also could be found in the previous assay.

Section S17. Calculation of Half Maximal Inhibitory Concentration (IC₅₀) for ChT

Herein, the IC₅₀ value is a quantitative measure that indicates how much of a particular inhibitor is needed to inhibit a given biological process by 50%. The value of it could be calculated by non-linear fitting using four-parameter logistic curves on Origin 2016 (Figure S14).⁷ The ChT activity was detected with the similar method as in section S4 and S5.

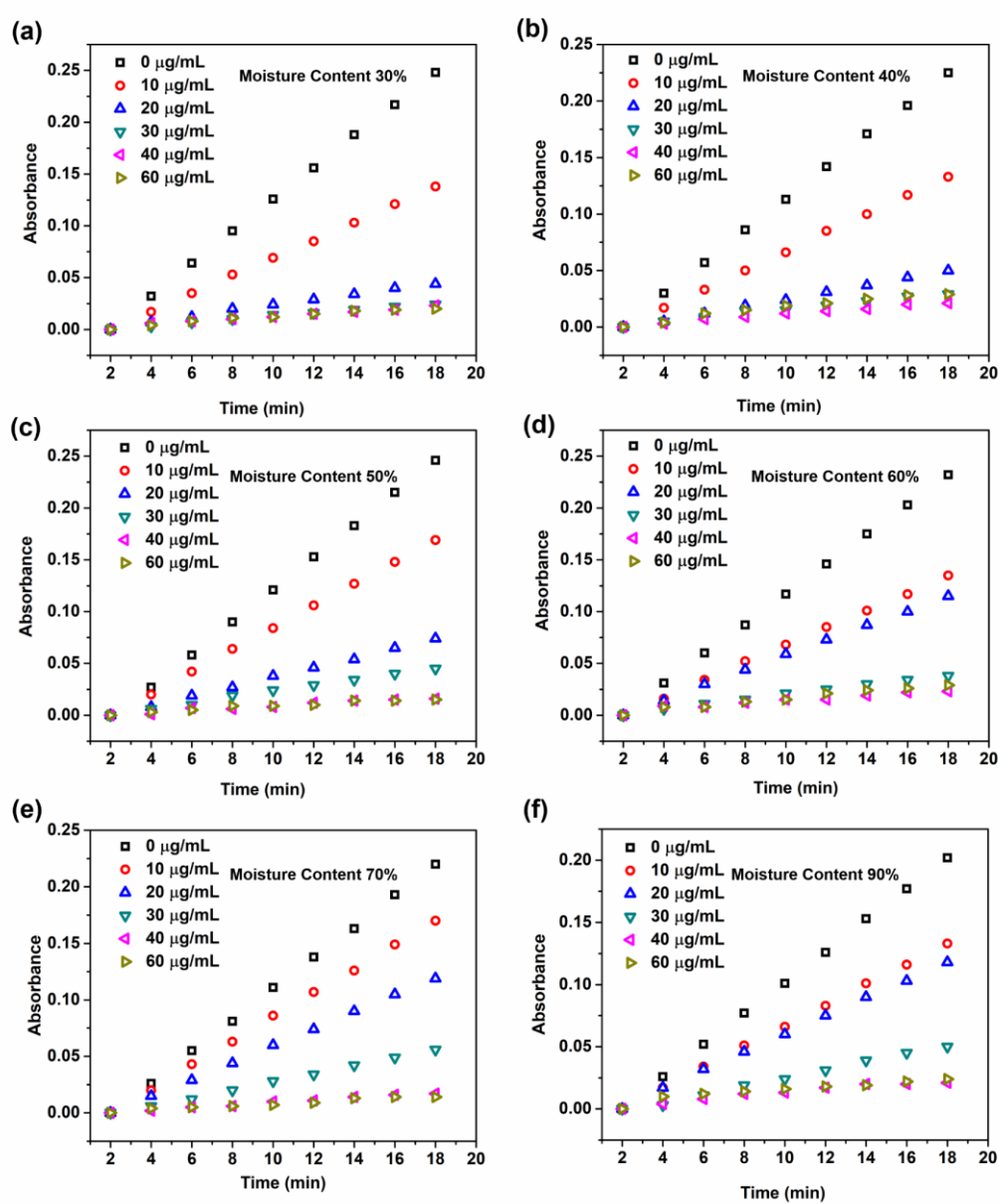


Figure S20. Activity of ChT (80 µg/mL) with different concentrations of HKUST-1 synthesized with water as modulators.

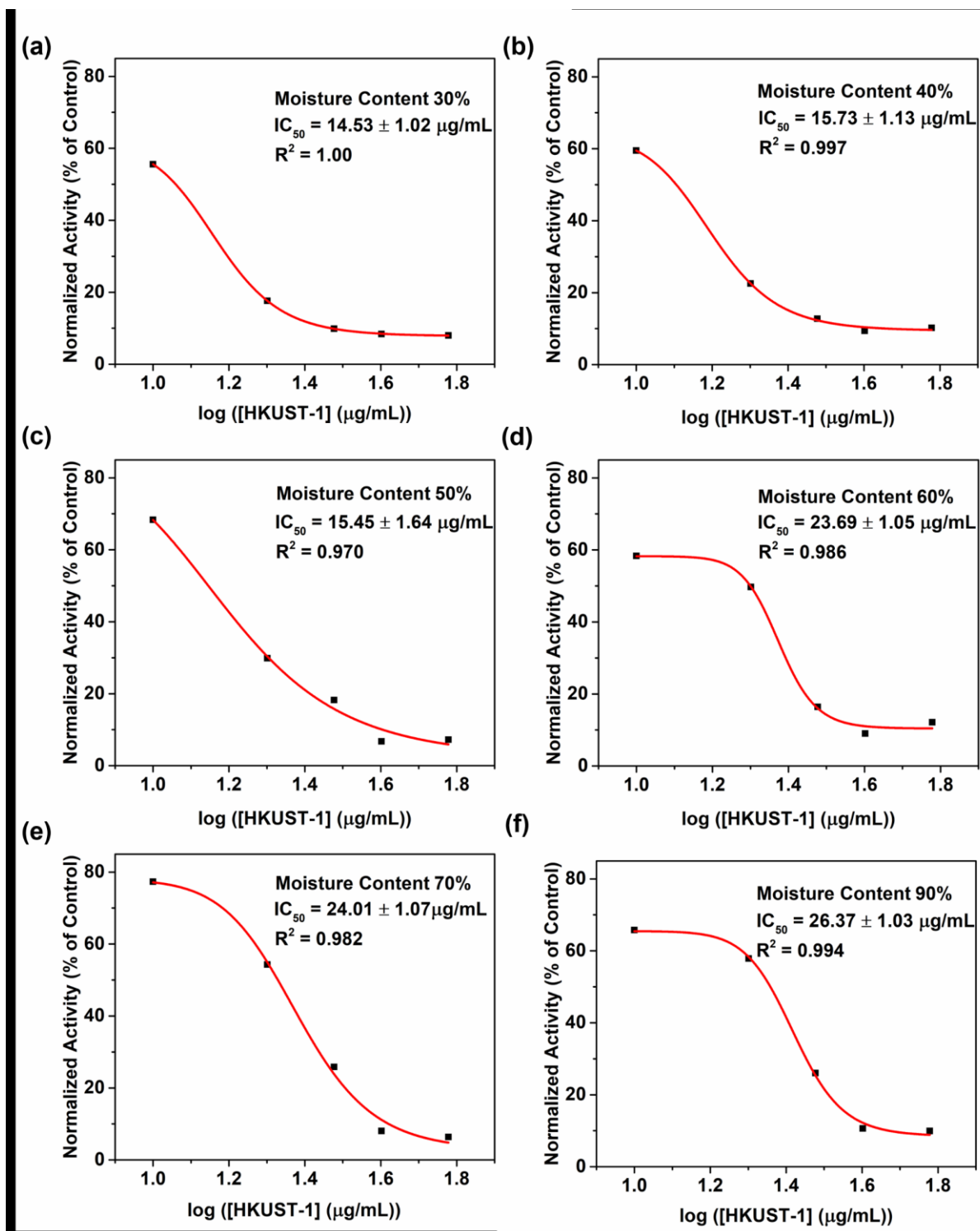


Figure S21. Calculations of the IC_{50} of different concentrations of HKUST-1 synthesized with water as modulators for 80 μg/mL ChT.

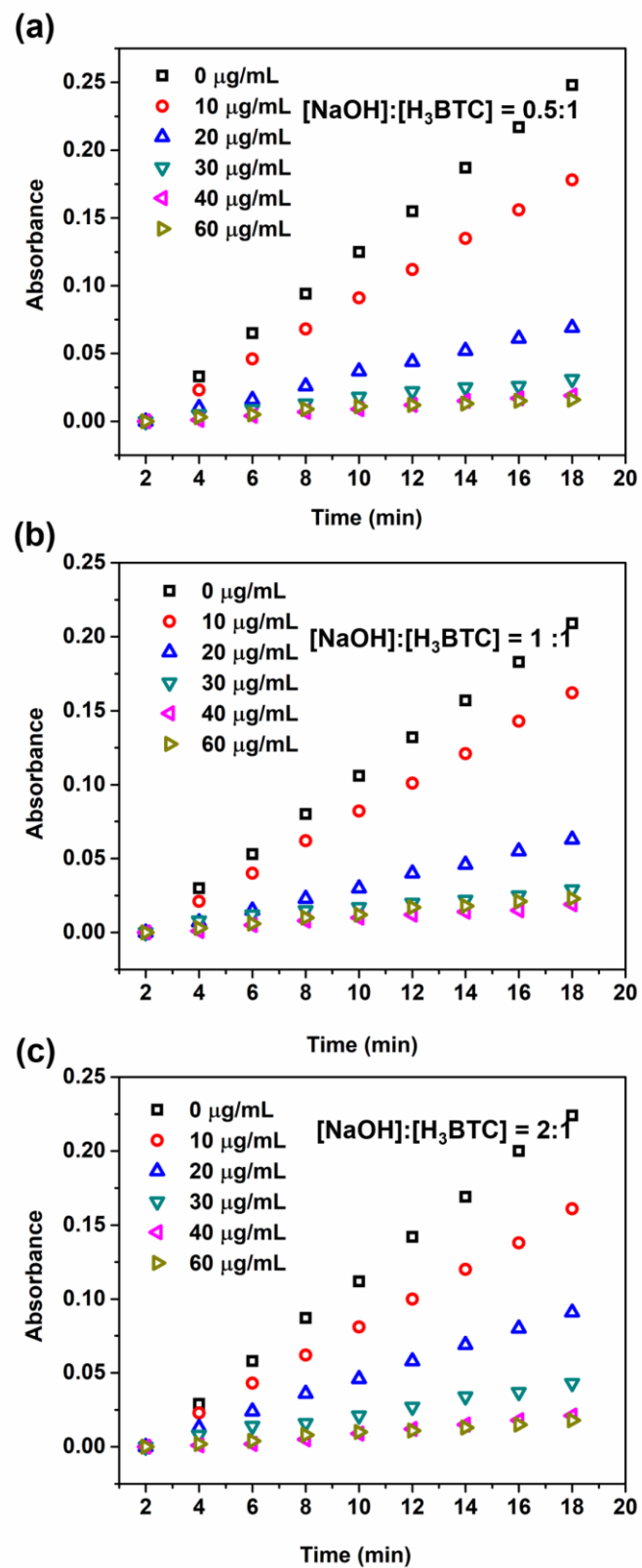


Figure S22. Activity of ChT (80 $\mu\text{g/mL}$) with different concentrations of HKUST-1 synthesized with NaOH as modulators.

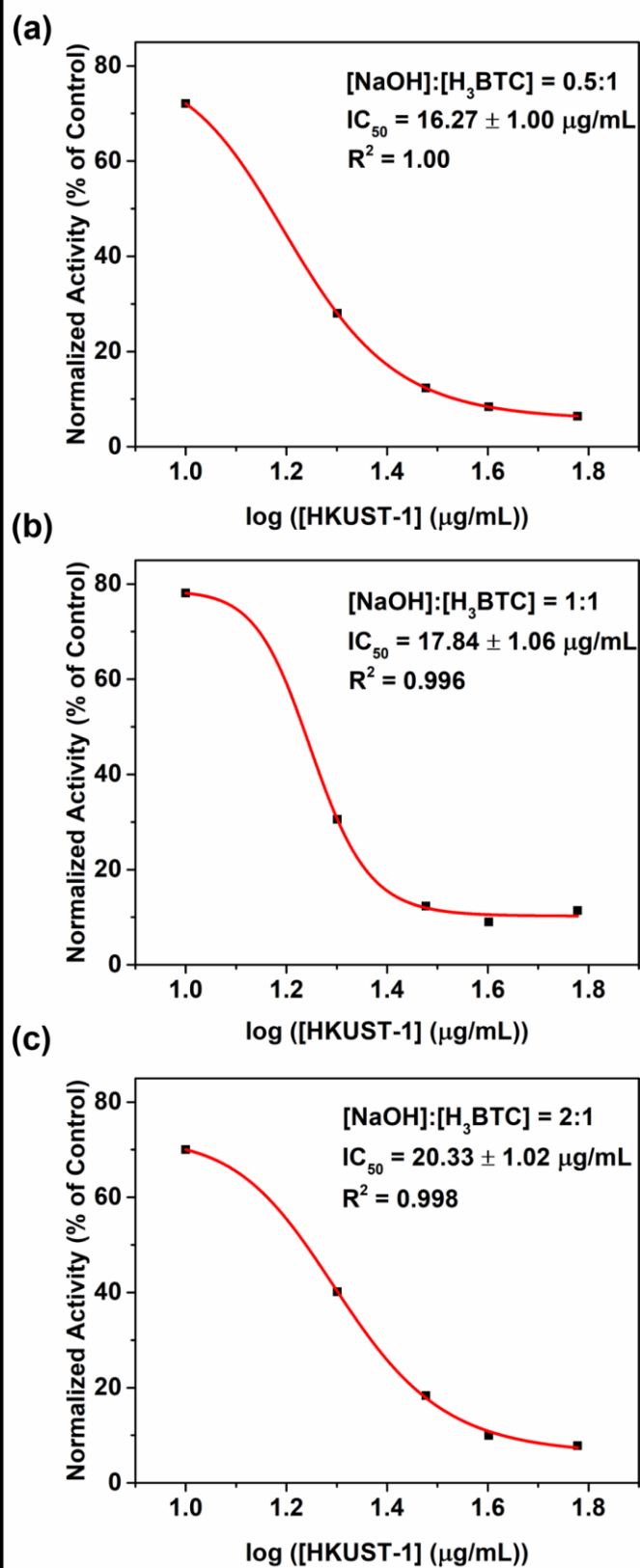


Figure S23. Calculations of the IC_{50} of different concentrations of HKUST-1 synthesized with NaOH as modulators for 80 $\mu\text{g/mL}$ ChT.

Section S18. Activity of ChT with the Incubation of BTC Ligands

ChT was dissolved in HEPPS buffer (100 mM, pH = 7.4). Different concentration of BTC ligands (0 and 30 $\mu\text{g/mL}$) was added into the ChT solution. Then, the mixture was kept standing in a 30 $^{\circ}\text{C}$ water bath for 10 min. The activity of ChT was detected.

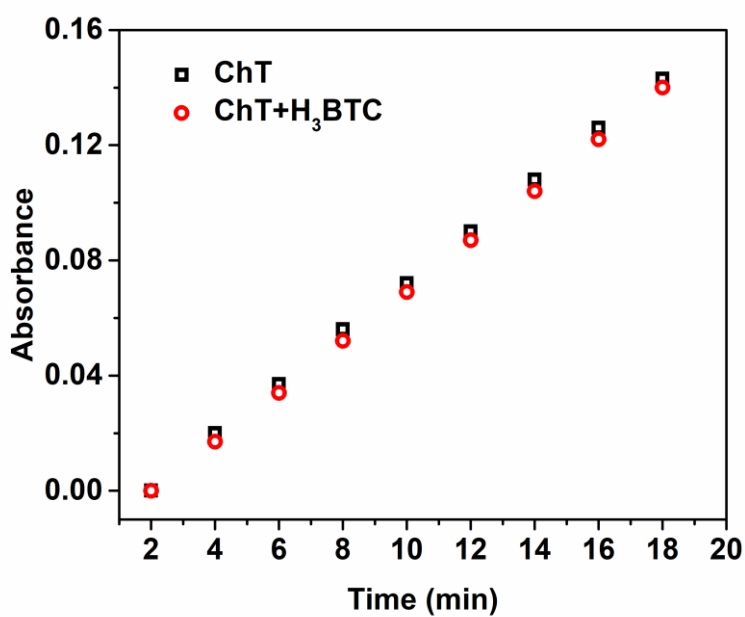


Figure S24. Activity of ChT (80 $\mu\text{g/mL}$) with and without the incubation of BTC ligands (30 $\mu\text{g/mL}$).

Reference

1. H. Assi, L. C. Pardo Pérez, G. Mouchaham, F. Ragon, M. Nasalevich, N. Guillou, C. Martineau, H. Chevreau, F. Kapteijn, J. Gascon, P. Fertey, E. Elkaim, C. Serre and T. Devic, Investigating the Case of Titanium(IV) Carboxyphenolate Photoactive Coordination Polymers *Inorg. Chem.*, 2016, **55**, 7192-7199.
2. M. Xu, L. Feng, L.-N. Yan, S.-S. Meng, S. Yuan, M.-J. He, H. Liang, X.-Y. Chen, H.-Y. Wei, Z.-Y. Gu and H.-C. Zhou, Discovery of Precise pH-Controlled Biomimetic Catalysts: Defective Zirconium Metal–Organic Frameworks as Alkaline Phosphatase Mimics *Nanoscale*, 2019, **11**, 11270-11278.
3. S.-N. Kim, J. Kim, H.-Y. Kim, H.-Y. Cho and W.-S. Ahn, Adsorption/Catalytic Properties of MIL-125 and NH₂-MIL-125 *Catal. Today*, 2013, **204**, 85-93.
4. A. Umemura, S. Diring, S. Furukawa, H. Uehara, T. Tsuruoka and S. Kitagawa, Morphology Design of Porous Coordination Polymer Crystals by Coordination Modulation *J. Am. Chem. Soc.*, 2011, **133**, 15506-15513.
5. K. Müller, J. Singh Malhi, J. Wohlgemuth, R. A. Fischer, C. Wöll, H. Gliemann and L. Heinke, Water as a Modulator in the Synthesis of Surface-Mounted Metal–Organic Framework Films of Type HKUST-1 *Dalton Trans.*, 2018, **47**, 16474-16479.
6. Q. Liu, J.-M. Yang, L.-N. Jin and W.-Y. Sun, Controlled Synthesis of Porous Coordination-Polymer Microcrystals with Definite Morphologies and Sizes under Mild Conditions *Chem. Eur. J.*, 2014, **20**, 14783-14789.
7. J. Prudhomme, E. McDaniel, N. Ponts, S. Bertani, W. Fenical, P. Jensen and K. Le Roch, Marine Actinomycetes: A New Source of Compounds against the Human Malaria Parasite *PLOS ONE*, 2008, **3**, e2335.